Switching in Nonminimum Phase Systems: Applications to a VSTOL Aircraft [1]

M. Oishi and C. Tomlin
Hybrid Systems Laboratory
Stanford University, Stanford, CA 94305
moishi,tomlin@stanford.edu

Abstract

We model the longitudinal dynamics of a VSTOL aircraft as a nonlinear hybrid system with three modes corresponding to typical aircraft behavior. Due to the nonminimum phase property of the aircraft, exact feedback linearization will not stabilize the aircraft. Using dynamic extension, approximate feedback linearization provides a stabilizing control in each mode. We show that the system will track with bounded error in each mode as well as across mode switches. Two examples of common VSTOL maneuvers demonstrate the effectiveness of the switched control scheme.

1 Introduction

A vectored-thrust Vertical and/or Short Take-Off and Landing (VSTOL) aircraft is an interesting example of a hybrid system with nonminimum phase dynamics. The McDonnell Douglas YAV-8B Harrier, described in [1, 2, 3] and pictured in Figure 1, has a wide range of maneuverability due to its vectored thrust, but is a difficult system to operate and to control: the pilot must manually control both the thrust and the nozzle angle with the same hand, stepping the nozzle through predefined angle sequences while adjusting the throttle accordingly. Researchers in the area of hybrid systems have been developing methods to simplify the analysis and control of complex continuous systems, by abstracting the system behavior into finite sets of modes within which the system is then easier to analyze and control [4, 5, 6]. A hybrid system model is particularly well suited to flight management systems on board modern commercial jets and military aircraft, as the autopilot modes in such systems typically coincide with aircraft behaviors in various flight regimes [7, 8, 9]. To simplify the inherent complexity of the system, we abstract the dynamic behavior of the aircraft into three

Figure 1: McDonnell Douglas YAV-8B Harrier

modes: a *conventional take-off and landing* (CTOL) mode, *vertical take-off and landing* (VTOL) mode, and *transition* (TRANSITION) mode.

The control problem is complicated by the fact that the hybrid system has nonlinear dynamics which are nonminimum phase. The nonlinear model allows a closer resemblance to the physical system, and accommodates tracking complicated trajectories. Much work has gone into developing control laws for the linearized dynamics of the aircraft [10, 11] using techniques such as gain scheduling. The tracking of nonminimum phase nonlinear systems has achieved successes in recent years with the development of control laws based on approximate linearization [12], on differential flatness [13], and on nonlinear stable inversion [14, 15].

In this paper, we first review our model, developed to study aerodynamic envelope protection [9]. We use approximate linearization to develop nonlinear control laws for the aircraft and show bounded tracking in each mode. We then prove stability of the system across switching boundaries and provide two examples of stable mode switching in typical VSTOL maneuvers.

2 Hybrid Model

We partition the aircraft dynamic behavior into three modes: CTOL mode in which the nozzles are at 0° relative to the horizontal body axis, VTOL mode in which the nozzles are at 90°, and TRANSITION mode in which the nozzles are between 0° and 90°.

[1]Research supported by a National Science Foundation Graduate Research Fellowship, Air Force (under F49620-97-1-0459), DARPA under the Software Enabled Control Program (administered by AFRL under contract F33615-99-C-3014), and a Stanford University Terman Faculty Award.

2.1 CTOL Mode

Consider the longitudinal axis dynamics of the VSTOL aircraft in CTOL mode. The horizontal and vertical axes are respectively the $(x_{inertial}, z_{inertial})$ (denoted x, z) axes and the *pitch angle* θ is the angle between the aircraft body axis, x_{body}, and the x axis. The *flight path angle* γ, the *angle of attack* α, and the *ground speed* V, are defined as $\gamma = \tan^{-1}(\frac{\dot{z}}{\dot{x}})$, $\alpha = \theta - \gamma$, and $V = \sqrt{\dot{x}^2 + \dot{z}^2}$, respectively. The aerodynamic equations for lift (L) and drag (D) of an aircraft are given by [16]

$$\begin{array}{rcl} L & = & a_L V^2(1 + c\alpha) \\ D & = & a_D V^2(1 + b(1 + c\alpha)^2) \end{array} \tag{1}$$

in which positive constants b, c, a_L, and a_D are determined from actual Harrier flight data [17]. Further details on the model development are available in [9].

We assume that the autopilot has direct control over both the forward thrust T and the aircraft pitch acceleration $\ddot{\theta}$ (through the elevators). We obtain the longitudinal dynamics from the Newton-Euler equations

$$M \begin{bmatrix} \ddot{x} \\ \ddot{z} \end{bmatrix} = R(\theta)\left(R^T(\alpha) \begin{bmatrix} -D \\ L \end{bmatrix} + \begin{bmatrix} T \\ -\epsilon u_2 \end{bmatrix}\right) - \begin{bmatrix} 0 \\ Mg \end{bmatrix} \tag{2}$$

where $R(\alpha)$ and $R(\theta)$ are standard rotation matrices, and ϵ is a small positive constant. The aircraft has mass $M = 16280$ lb and moment of inertia around the pitch angle $J = 32000$ slug-ft^2. In CTOL mode, we use $b = 0.002$, $c = 39.97$, $a_L = 0.78$, $a_D = 2.62$.[1]

2.2 VTOL Mode

In VTOL mode, the ground speed is low enough that we assume the aerodynamic lift and drag forces are negligible. The dynamics simplify from (2) to:

$$M \begin{bmatrix} \ddot{x} \\ \ddot{z} \end{bmatrix} = R(\theta) \begin{bmatrix} 0 \\ T - \epsilon u_2 \end{bmatrix} - \begin{bmatrix} 0 \\ Mg \end{bmatrix} \tag{3}$$

2.3 TRANSITION Mode

We introduce the additional states δ and $\dot{\delta}$, which model the dynamics of the nozzles, and a third control variable, $u_3 = \ddot{\delta}$. Continuity of the physical system only allows switching between TRANSITION and CTOL when $(\delta, \dot{\delta}) = (0, 0)$; likewise, between TRANSITION and VTOL when $(\delta, \dot{\delta}) = (\pi/2, 0)$. The thrust input is affected by a non-zero δ:

$$M \begin{bmatrix} \ddot{x} \\ \ddot{z} \end{bmatrix} = R(\theta) \left(R^T(\alpha) \begin{bmatrix} -D \\ L \end{bmatrix} + \begin{bmatrix} T\cos\delta \\ T\sin\delta - \epsilon u_2 \end{bmatrix}\right) - \begin{bmatrix} 0 \\ Mg \end{bmatrix} \tag{4}$$

In TRANSITION mode, $b = 0.02$, $c = 11.42$, $a_L = 2.72$, $a_D = 2.54$.

[1] While most of the parameters were extracted from information in [1, 2, 3, 17], some are our estimates.

3 Approximate Tracking in Three Flight Regimes

The VSTOL aircraft is nonminimum phase due to the $\epsilon-$coupling between the pitch moment and the downward acceleration [12]. In this section, we design nonlinear tracking control laws for the aircraft in all three modes based on the approximate linearization method of [12], which will guarantee order ϵ bounded tracking of desired trajectories y_d within each mode. By assuming $\epsilon/M \approx 0$, the input $u_2 = J\ddot{\theta}$ will not appear in the second derivatives of the outputs. Dynamically extending the state to include T and $\dot{T}$, the new input for the extended system is $u_1 = \ddot{T}$.

3.1 CTOL Mode

As shown in [18], exact linearization from outputs $y_1 = x$ and $y_2 = z$ to inputs T and $J\ddot{\theta}$ produces unstable zero dynamics:

$$\ddot{\theta} = \frac{1}{J\epsilon}\left(D\sin\theta + L\cos\theta - Mg\cos\theta\right). \tag{5}$$

Approximate linearization rids the extended system of internal dynamics [12]. We transform the original state $\underline{x} = [\ x \quad \dot{x} \quad z \quad \dot{z} \quad \theta \quad \dot{\theta} \quad T \quad \dot{T}\ ]^T$ to the approximate state $\tilde{\xi} = [\ \tilde{\xi}_1^1 \quad \tilde{\xi}_2^1 \quad \tilde{\xi}_3^1 \quad \tilde{\xi}_4^1 \quad \tilde{\xi}_1^2 \quad \tilde{\xi}_2^2 \quad \tilde{\xi}_3^2 \quad \tilde{\xi}_4^2\ ]^T$, where $\tilde{\xi}_1^1 = x$, $\tilde{\xi}_1^2 = z$, $\tilde{\xi}_2^1 = \dot{x}$, $\tilde{\xi}_2^2 = \dot{z}$,

$$M \begin{bmatrix} \tilde{\xi}_3^1 \\ \tilde{\xi}_3^2 \end{bmatrix} = R(\theta)\left(R^T(\alpha) \begin{bmatrix} -D \\ L \end{bmatrix} + \begin{bmatrix} T \\ 0 \end{bmatrix}\right) - \begin{bmatrix} 0 \\ Mg \end{bmatrix},$$

$\tilde{\xi}_4^1 = \dot{\tilde{\xi}}_3^1$, and $\tilde{\xi}_4^2 = \dot{\tilde{\xi}}_3^2$, not written out in full for brevity.

The exact system can be written in approximate system coordinates by adding the ϵ-terms to the second derivatives. The Lie derivatives $L_f^4 h_i, L_{g1}L_f^3 h_i, L_{g2}L_f^3 h_i$, $i \in \{1, 2\}$ are defined in the standard manner [19]:

$$\begin{array}{rcl} \dot{\tilde{\xi}}_1^1 & = & \tilde{\xi}_2^1 \\ \dot{\tilde{\xi}}_2^1 & = & \tilde{\xi}_3^1 + \epsilon\left(\frac{\sin\theta}{M}\right) u_2 \\ \dot{\tilde{\xi}}_3^1 & = & \tilde{\xi}_4^1 \\ \dot{\tilde{\xi}}_4^1 & = & L_f^4 h_1 + L_{g1}L_f^3 h_1 u_1 + L_{g2}L_f^3 h_1 u_2 \\ \dot{\tilde{\xi}}_1^2 & = & \tilde{\xi}_2^2 \\ \dot{\tilde{\xi}}_2^2 & = & \tilde{\xi}_3^2 + \epsilon\left(-\frac{\cos\theta}{M}\right) u_2 \\ \dot{\tilde{\xi}}_3^2 & = & \tilde{\xi}_4^2 \\ \dot{\tilde{\xi}}_4^2 & = & L_f^4 h_2 + L_{g1}L_f^3 h_2 u_1 + L_{g2}L_f^3 h_2 u_2 \end{array} \tag{6}$$

The feedback linearizing control $u^*(\underline{x})$ for the approximate system results in $[\ \dot{\tilde{\xi}}_4^1 \quad \dot{\tilde{\xi}}_4^2\ ]^T = [\ v_1 \quad v_2\ ]^T$, where v_1 and v_2 are auxiliary inputs determined from a linear control law designed to zero the output tracking error $e = \tilde{\xi} - y_d$. This produces asymptotically stable

error dynamics $\dot{e} = Ae$, where $A = \text{diag}\{A_1, A_2\}$.

$$A_1 = \begin{bmatrix} 0 & 1 & 0 & 0 \\ 0 & 0 & 1 & 0 \\ 0 & 0 & 0 & 1 \\ -\alpha_0^1 & -\alpha_1^1 & -\alpha_2^1 & -\alpha_3^1 \end{bmatrix} A_2 = \begin{bmatrix} 0 & 1 & 0 & 0 \\ 0 & 0 & 1 & 0 \\ 0 & 0 & 0 & 1 \\ -\alpha_0^2 & -\alpha_1^2 & -\alpha_2^2 & -\alpha_3^2 \end{bmatrix} \quad (7)$$

The desired error dynamics are given as in [18], by

$$(s + \lambda_e)^4 = s^4 + \alpha_3 s^3 + \alpha_2 s^2 + \alpha_1 s + \alpha_0 \quad (8)$$

with $\lambda_e = 1.3$, and $\alpha_j^1 = \alpha_j^2 = \alpha_j, j \in \{0, 1, 2, 3\}$. This same control, applied to the exact system, results in the error dynamics

$$\dot{e} = Ae + \epsilon\psi(\underline{x})u^*(\underline{x}) \quad (9)$$

$$\psi(\underline{x})^T = \begin{bmatrix} 0 & 0 & 0 & 0 & 0 & 0 & 0 & 0 \\ 0 & \frac{\sin\theta}{M} & 0 & 0 & 0 & -\frac{\cos\theta}{M} & 0 & 0 \end{bmatrix} \quad (10)$$

Since the approximate system has no zero dynamics, the Hauser-Sastry-Meyer Theorem for the exact system (6) in tracking (9) can be written as follows:

Theorem 1 (Hauser-Sastry-Meyer [12]) *Suppose that $\psi(\underline{x})u^*(\underline{x})$ is locally Lipschitz continuous. Then for ϵ sufficiently small and for desired trajectories with sufficiently small values and derivatives, the states of the exact system will be bounded and the tracking errors will be bounded as:*

$$\begin{aligned} |e_1| &= |\tilde{\xi}_1^1 - y_{d1}| \leq k\epsilon \\ |e_2| &= |\tilde{\xi}_1^2 - y_{d2}| \leq k\epsilon \end{aligned} \quad (11)$$

for some $k < \infty$.

Assuming that $L_f^4 h_1$ and $L_f^4 h_2$ are locally Lipschitz, we can also show that $\psi(\underline{x})u^*(\underline{x})$ is locally Lipschitz. With these two conditions, according to Theorem 1, the exact system produces bounded tracking for sufficiently small ϵ.

Remark 1 *While guaranteeing bounded tracking, this derivation does not give an indication of the region of attraction of the system. Through simulations we have found the system very robust to various initial conditions away from the desired trajectory.*

3.2 VTOL Mode

The system is not exactly linearizable since the linearizing controls require inverting a matrix which is always singular. To avoid this, approximate linearization is implemented as in [12] with extended system inputs. As in CTOL, taking derivatives of the outputs $y_1 = x$ and $y_2 = z$ results in the approximate system $\tilde{\xi} = [x, \dot{x}, -\frac{T}{M}\sin\theta, \frac{1}{M}(-T\dot{\theta}\cos\theta - \dot{T}\sin\theta), z, \dot{z}, \frac{T}{M}\cos\theta - g, \frac{1}{M}(-T\dot{\theta}\sin\theta + \dot{T}\cos\theta)]$. Using dynamic inversion, the resulting feedback law is

$$\begin{bmatrix} u_1^* \\ u_2^* \end{bmatrix} = \begin{bmatrix} \dot{\theta}^2 T \\ -\frac{2J\dot{\theta}\dot{T}}{T} \end{bmatrix} + M \begin{bmatrix} -\sin\theta & \cos\theta \\ -\frac{J\cos\theta}{T} & -\frac{J\sin\theta}{T} \end{bmatrix} \begin{bmatrix} v_1 \\ v_2 \end{bmatrix} \quad (12)$$

with reference inputs v_1 and v_2 chosen so that the error dynamics of the exact system follow (9). As in CTOL, A and $\psi(\underline{x})$ are given by (7), (8), and (10). Again, by Theorem 1, this control law produces bounded tracking for the original system.

3.3 TRANSITION Mode

As in CTOL mode, the system has unstable zero dynamics when exact linearization is used.

$$\ddot{\theta} = \frac{1}{J\epsilon}\left(D(\sin\theta + \cos\theta\tan\delta) + L(\cos\theta - \sin\theta\tan\delta) + Mg(-\cos\theta + \sin\theta\tan\delta)\right) \quad (13)$$

The approximate linearization of the extended system does not produce any internal dynamics. With two additional states, choosing outputs $y_1 = x$, $y_2 = z$, and $y_3 = \delta$ results in the approximate system coordinates $\tilde{\xi} = [\ \tilde{\xi}_1^1\ \ \tilde{\xi}_2^1\ \ \tilde{\xi}_3^1\ \ \tilde{\xi}_4^1\ \ \tilde{\xi}_1^2\ \ \tilde{\xi}_2^2\ \ \tilde{\xi}_3^2\ \ \tilde{\xi}_4^2\ \ \tilde{\xi}_1^3\ \ \tilde{\xi}_2^3\ ]$. Using dynamic inversion, the system is linearized from its external inputs to its approximated outputs through $[\dot{\tilde{\xi}}_4^1\ \ \dot{\tilde{\xi}}_4^2\ \ \dot{\tilde{\xi}}_2^3]$. We again choose to place the error dynamics according to (9), where $A = \text{diag}(A_1, A_2, A_3)$ and $\psi(\underline{x})$ are extended to accommodate the additional input and states in TRANSITION mode.

$$A_3 = \begin{bmatrix} 0 & 1 \\ -\alpha_0^3 & -\alpha_1^3 \end{bmatrix}$$

$$\psi^T(\underline{x}) = \begin{bmatrix} 0 & 0 & 0 & 0 & 0 & 0 & 0 & 0 \\ 0 & \frac{\sin\theta}{M} & 0 & 0 & 0 & -\frac{\cos\theta}{M} & 0 & 0 \\ 0 & 0 & 0 & 0 & 0 & 0 & 0 & 0 \end{bmatrix} \quad (14)$$

Again, with $\lambda_e = 1.3$, $\alpha_j^1 = \alpha_j^2 = \alpha_j$ as in CTOL (7,8). Additionally, the error dynamics of y_3 are given by

$$(s + \lambda_d)^2 = s^2 + \alpha_1^3 s + \alpha_0^3 \quad (15)$$

where $\lambda_d = 1.3$. Again, Theorem 1 proves order ϵ bounded tracking for the exact system.

4 Switching Stability

We have shown through the Hauser-Sastry-Meyer Theorem that the tracking error within each mode converges to a ball of order ϵ. Forming the error dynamics equation in each mode as a linear system driven by an input of order ϵ results in a solution which is close to the exponential solution of the linear approximation, $\dot{e} = Ae$. We now prove stability of the system across switching boundaries, using a Lyapunov stability argument between modes.

A family of systems $\dot{x} = f_p(x), p \in P$ where P is a set of indices, is stable if there exists a common Lyapunov function $v(x, t)$ for all $x \neq 0$ and all $p \in P$ [20]. We show local stability of our family of error dynamics by proving that $v(e, t) > 0$ and $\dot{v}(e, t) \leq 0$ for all e in a neighborhood of 0. We additionally show $\dot{v}(e, t) < 0$ for large $|e|$.

Corollary 1 *The family of systems (2),(3),(4) using approximate feedback linearization tracks a desired trajectory with order ϵ bounded error.*

Proof: Augment the state and input vectors in CTOL and VTOL modes to include δ and $\dot{\delta}$ as well as $u_3 = \ddot{\delta}$, as in TRANSITION mode. The additional transformed state equations are $\dddot{\xi}_1^3 = 0$ and $\dddot{\xi}_2^3 = 0$ in both modes.

Since the error dynamics in each mode were explicitly chosen to have the same pole locations, the resulting A for the error equation (9) is the same in CTOL, VTOL, and TRANSITION modes. In the manner of the Hauser-Sastry-Meyer proof, choose a candidate Lyapunov function

$$v(e,t) = e^T P e \tag{16}$$

in which $P > 0$ satisfies

$$A^T P + PA = -I. \tag{17}$$

Recall that in each mode:

- the desired trajectory y_d and its derivatives are bounded.
- $\psi(\underline{x})u^*(\underline{x})$ is locally Lipschitz continuous.

Then

$$\begin{array}{rcl} |\tilde{\xi}| & \leq & |e| + b_d \\ |2P\psi(\underline{x})u^*(\underline{x})| & \leq & l_u|\underline{x}| \\ |\underline{x}| & \leq & l_x|\tilde{\xi}| \end{array} \tag{18}$$

directly follows. Take the derivative of (16) along the trajectories of (9).

$$\begin{array}{rcll} \dot{v}(e,t) & = & e^T P\dot{e} + \dot{e}^T P e & \\ & = & -|e|^2 + 2e^T P\epsilon\psi(\underline{x})u^*(\underline{x}) & \\ & \leq & -|e|^2 + \epsilon l_u l_x |e|(|e| + b_d) & \text{using (18)} \\ & \leq & -\left(\frac{|e|}{2} - \epsilon l_u l_x b_d\right)^2 + (\epsilon l_u l_x b_d)^2 & \\ & & \qquad -\frac{|e|}{4}^2 - \left(\frac{1}{2} - \epsilon l_u l_x\right)^2 & \end{array}$$

Now for $\epsilon < \frac{1}{4l_u l_x}$,

$$\dot{v}(e,t) \leq -\tfrac{1}{4}|e|^2 + (\epsilon l_u l_x b_d)^2$$

Therefore $\dot{v}(e,t) < 0$ when $|e|$ is large (to ensure $\epsilon < \frac{1}{4l_u l_x}$). Since $v(e,t) > 0$ and $\dot{v}(e,t) \leq 0$, the tracking error e is bounded. ■

5 Automatic Mode Sequencing Examples

We demonstrate the stability of our switched system with two maneuvers used by VSTOL aircraft: the *short take-off* and the *vertical landing* maneuvers.

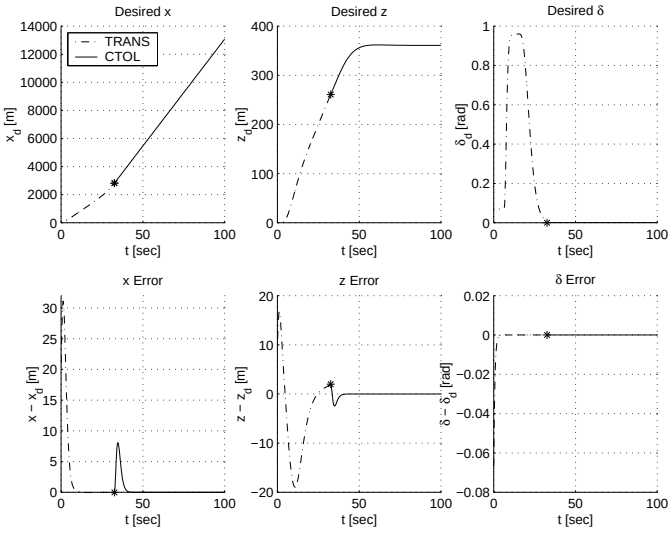

Figure 2: Short Take-Off Maneuver

In the *short take-off maneuver*, the autopilot raises the nozzle angle δ sharply to a preset value of 55°, which coincides with the plane's take-off, then gradually rotates the nozzle aft as speed increases and the plane transitions from jet-born to wing-born flight [3]. Modeling this as a switch from TRANSITION mode to CTOL mode, the switch is requested after the nozzles are fully rotated aft and the velocity is above 100 m/s. Matching pilot data from [3], $\dot{x}_d$ is a third-order polynomial and the $\dot{z}_d$ trajectory follows the dynamics of

$$\begin{aligned} 0 = \dot{z}_d^{(5)} + g_4\dot{z}_d^{(4)} + g_3\dot{z}_d^{(3)} + g_2\dot{z}_d^{(2)} \\ + g_1\dot{z}_d^{(1)} + g_0(\dot{z}_d - Z_f) \end{aligned} \tag{19}$$

with a final velocity $Z_f = 8$ m/s before the switch. The g_i are the coefficients of the polynomial $(s + \lambda_g)^5$, where $\lambda_g = 0.5882$. The δ trajectory rises to 55° in 2 seconds, then returns to 0° over 10 seconds, as shown in Figure 2. After switching to CTOL mode, the aircraft levels out to a constant altitude and constant $\dot{x}$. The initial conditions are initially offset from the desired trajectory, but the error trajectories rapidly converge to 0. The switch generates deviations from the desired trajectories due to the discontinuities in the desired trajectories as well as in the control law across the switch.

In the *vertical landing* maneuver, the autopilot again steps the nozzle angle δ through various predetermined set-points while slowing to a hover. In the final segment of the maneuver (Figure 3), the nozzle steadily increases from 65° to 90° as $\dot{x}_d$ decreases. The aircraft switches to VTOL mode once the velocity is below 20 m/s and the nozzle is rotated to 90°. In VTOL mode, the aircraft maintains its forward velocity while decreasing its altitude by 50 meters over 50 seconds. The system tracks very well, with errors less than 1 meter in the x and z trajectories.

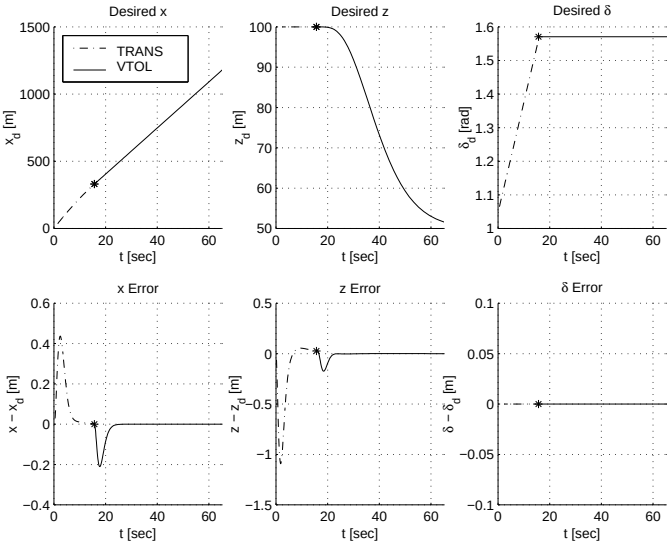

Figure 3: Vertical Landing Maneuver

6 Conclusion and Future Work

The VSTOL aircraft is well-suited to a switched-system formulation. In this three-mode system we proved tracking with bounded error in each mode using an approximate feedback linearizing controller. We found a common Lyapunov function by carefully choosing the desired error dynamics in each mode. We then proved the stability of our switched system by verifying the candidate Lyapunov function. Two simulations of common VSTOL maneuvers show successful tracking across two switching boundaries. While we still have no formal definition of the region of attraction for this local stability result, simulations have shown the system has quite a large tolerance for initial deviations from the desired trajectory.

In the future, we would like to incorporate this work into a full, computable hybrid model. We would also like to continue with our work on the safety of the aircraft [9], combining these tracking results with further control restrictions to provide tracking while ensuring the aircraft remains within an allowable region of operation.

References

[1] B. David McNally. Full-envelope aerodynamic modeling of the Harrier Aircraft. NASA Technical Memorandum 88376, 1985.

[2] J. A. Franklin, M. W. Stortz, P. F. Borchers, and E. Moralez. Flight evaluation of advanced controls and displays for transition and landing on the NASA VSTOL systems research aircraft. NASA Technical Paper 3607, 1996.

[3] J. Fozard. British Aerospace Harrier case study in aircraft design. AIAA Publication Series, 1978.

[4] M.S. Branicky. *Control of Hybrid Systems*. PhD thesis, Department of Electrical Engineering and Computer Sciences, Massachusetts Institute of Technology, 1994.

[5] Datta N. Godbole and John Lygeros. Longitudinal control of the lead car of a platoon. *IEEE Transactions on Vehicular Technology*, 43(4):1125–1135, 1994.

[6] J. Lygeros, C. Tomlin, and S. Sastry. Controllers for reachability specifications for hybrid systems. *Automatica*, 35(3), 1999.

[7] G. Meyer. Design of flight vehicle management systems. Plenary Talk at the IEEE Conference on Decision and Control, 1994.

[8] C. Tomlin, J. Lygeros, and S. Sastry. Aerodynamic envelope protection using hybrid control. In *Proceedings of the American Control Conference*, pages 1793–1796, Phildelphia, PA, 1998.

[9] M. Oishi and C. Tomlin. Switched nonlinear control of a VSTOL aircraft. In *Proceedings of the IEEE Conference on Decision and Control*, 1999.

[10] J. A. Franklin. Control of V/STOL aircraft. *Aeronautical Journal*, 90(895):157–173, 1986.

[11] R.A. Hyde. *H_∞ Aerospace Control Design: A VSTOL Flight Application*. Springer-Verlag, London, 1995.

[12] J. Hauser, S. Sastry, and G. Meyer. Nonlinear control design for slightly nonminimum phase systems: Application to V/STOL aircraft. *Automatica*, 28(4):665–679, 1992.

[13] P. Martin, S. Devasia, and B. Paden. A different look at output tracking: control of a VTOL aircraft. In *Proceedings of the IEEE Conference on Decision and Control*, pages 2376–2381, San Antonio, TX, 1994.

[14] S. Devasia, D. Chen, and B. Paden. Nonlinear inversion-based output tracking. *IEEE Transactions on Automatic Control*, 41(7):930–942, 1996.

[15] C. Tomlin and S. Sastry. Bounded tracking for nonminimum phase nonlinear systems with fast zero dynamics. *International Journal of Control*, 68(4):819–847, 1997.

[16] B. W. McCormick. *Aerodynamics, Aeronautics, and Flight Mechanics*. John Wiley and Sons, Inc., 1995.

[17] YAV-8B Simulation and Modeling. Technical Report CR-170397, NASA, March 1983.

[18] C. Tomlin, J. Lygeros, L. Benvenuti, and S. Sastry. Output tracking for a non-minimum phase dynamic CTOL aircraft model. In *Proceedings of the IEEE Conference on Decision and Control*, 1995.

[19] S. S. Sastry. *Nonlinear Systems: Analysis, Stability and Control*. Springer-Verlag, 1999.

[20] D. Liberzon and A. S. Morse. Basic problems in stability and design of switched systems. *IEEE Control Systems Magazine*, 19(5):59–70, October 1999.